Titanium dioxide-carbon nanotubes hybrid to simultaneously achieve mechanical enhancement of natural rubber and its high-temperature stability under extreme friction condition

Le Wan, Cong Deng*, Ze-Yong Zhao, Hai-Bo Zhao, Yu-Zhong Wang

The Collaborative Innovation Center for Eco-Friendly and Fire-Safety Polymeric Materials, National Engineering Laboratory of Eco-Friendly Polymeric Materials (Sichuan), State Key Laboratory of Polymer Materials Engineering, Analytical & Testing Center, Sichuan University, Chengdu 610064, China

Abstract: Currently, carbon black as an efficient reinforcing agent dominates the reinforcement field of natural rubber (NR). However, its general loading amount is quite high in achieving the reinforcement of NR. In this work, titanium oxide-carbon nanotubes (TiO_2-CNTs) were prepared by using the hydrothermal method. When a small amount of TiO_2-CNTs additive was used to reinforce NR, significantly mechanical enhancement was achieved. Experimental result confirmed that the tensile strength and elongation at break of NR containing 3.0 wt% TiO_2-CNTs (NR/3TiO_2-CNTs) was 32.0 MPa and 1604%, respectively, corresponding increased by 79.5% and 14.5% in comparison with that of pristine NR. Moreover, thermal analysis confirmed that the initial decomposing temperature of NR was promoted to 313.5 ℃ from 287.9 ℃ after incorporation of only 3 wt% TiO_2-CNTs, raised by 25.6 ℃. An intensive friction test confirmed that the maximum temperatures at the surfaces of NR/3TiO_2-CNTs and NR/5TiO_2-CNTs were 217 and 210 ℃, respectively decreased by 29 and 36 ℃ in comparison with that of NR. The study for mechanical enhancement confirmed that the uniform dispersion of TiO_2-CNTs and superior interfacial interactions between NR and TiO_2-CNTs played a dominant role for the mechanical enhancement of NR/TiO_2-CNTs composites. For the improved high-temperature stability of NR/TiO_2-CNTs composites, the physical barrier action of TiO_2-CNTs to heat and oxygen, excellent

*Corresponding author: Cong Deng
E-mail address: dengcong@scu.edu.cn (C. Deng).

heat dispersion of CNTs, and the increased graphitization degree at the surface played a vital role. The TiO_2-CNTs show specific advantages in simultaneously reinforcing mechanical properties of NR and promoting its high-temperature stability under extreme friction condition.

Keywords: natural rubber; carbon nanotube; titanium dioxide; thermal stability; mechanical property

1. Introduction

The working environment of aircraft tires is very harsh during landing, including high speed, high load, high temperature, and intensive friction. In this case, the temperature at the tread of aircraft tires will rise sharply, and the instantaneous temperature can reach 300-400 ℃, which causes the tread of aircraft tires to be damaged easily, and this kind of damage will bring a great threat to the safety of human beings and aircrafts. In current work, carbon black is usually applied to reinforce NR. As an efficient reinforcing agent, carbon black dominates the reinforcing field of NR. Moreover, it has also been confirmed that carbon black-reinforced NR possesses high thermal stability. Matheson et al. [1], studied the effect of carbon black on the thermally decomposing behavior of NR, and the results showed that the presence of carbon black did not apparently bring any negative affect on the thermal stability of NR. Although the carbon black has its own advantages in reinforcing NR, the high loading amount of carbon black is a shortcoming in the case of fulfilling the requirements in mechanical, high-temperature stability, and other properties in fabricating the tread material of aircraft tires.

In order to prepare NR composites with excellent mechanical properties and high-temperature stability, many researchers had done much work. In terms of the thermal stability of NR composites, some researchers deeply investigated the thermal decomposition behavior of NR and further explored some novel NR-based composites. Straus et al. [2], studied the thermal decomposition behavior of vulcanized rubber under vacuum condition, and they found that the crosslinking bond was easy to break at the pyrolysis temperature, and then the effect of crosslinking became invalid at higher temperature.

Ginger et al. [3], studied the thermal decomposition behavior of crosslinked polyisoprene and found that the molecular chain rearranged and resulted in the formation of terminal double bond during heating. In addition, due to the crosslinking, both thermal stability and thermal-oxidation stability were enhanced. For NR, both vulcanization and crosslinking may affect the type and yield of the thermal decomposition products. Generally, the yield of the produced monomers and dimers will decrease with increasing the crosslinking density, but the yield of 3-methyl-1,3-pentylene will not remarkably fluctuate with the change of crosslinking density [4-6]. Chen et al. [7], pyrolyzed cis-1,4-polyisoprene in different temperature ranges, and the results showed that the concentrations of isoprene and dipentene formed at relatively low temperature were higher. At relatively high temperature, a high yield of hydrocarbon was obtained due to intensive decomposition of polymer [8-10].

On the basis of above fundamental research, some novel NR-based composites with improved thermal stability and mechanical properties were developed, in which nanoparticles have been proved to be very efficient to achieve the improved thermal properties. Here, nanoparticles mainly contain carbon nanotubes, modified montmorillonite (MMT), silica, calcium carbonate, carbon black, and starch, etc. Khanlari et al. [11], used the modified MMT to promote the thermal stability of NR. The result confirmed that the thermal decomposition of MMT-filled nanocomposites shifted towards the higher temperature range, and the temperatures at 20 and 50 wt% mass loss were increased by 20 and 15 ℃, respectively. Among different types of nanofillers, CNTs have also been demonstrated to be very efficient in improving the thermal stability and mechanical properties of NR. Fakhru' I-Razi et al. found that the high strain value was obtained for the nanocomposite with 1.0 wt% CNTs. Moreover, better heat dispersion and higher thermal stability were simultaneously achieved for NR/CNTs nanocomposites. However, due to the fact that CNTs are easy to agglomerate and entangle, it is difficult to uniformly disperse in the matrix [12, 13]. In addition, it has been confirmed that TiO_2 nanoparticles

can improve the thermal stability and high temperature resistance of polymers. Hayeemasae et al. [14] found TiO_2 nanoparticles had an apparent influence on the thermal stability of NR. The results showed that the decomposition temperatures at 10 and 50% weight loss for NR composite were remarkably raised when a small amount of TiO_2 was added in the NR composite.

According to a previous report [15], compared with mono-component filler, the synergy of two or more kinds of reinforcing materials can improve the dispersion of fillers and meanwhile endow rubber better specific properties or better comprehensive properties. Therefore, a joint action of CNTs and TiO_2 might have a positive influence on the mechanical enhancement and thermal stability of NR. In this work, the TiO_2-CNTs was prepared by sol-gel method and used to fabricate NR/TiO_2-CNTs composite via the latex composite method to fabricate the NR composites with excellent comprehensive properties. [16] The mechanical properties and high-temperature stability of NR composites were investigated with the aid of different measurement. Moreover, the corresponding mechanisms for the improved mechanical properties and high-temperature stability were discussed in detail.

2. Experimental Section

2.1. Materials

NR was purchased from Tianjin Changli Rubber Co., Ltd (China), the Dry rubber content (DRC) of NR is about 60%; carbon black (CB, N330) was supplied by Cabot Corporation (USA); Carbon nanotubes (TNSMC3, hydroxylation, industrial grade) were provided by Institute of Organic Chemistry (Chinese Academy of Sciences), and their outer diameter and length are about 10-20 nm and 0.5-2.0 μm, respectively; Anhydrous ethanol (analytical reagent), titanium isopropanol (analytical reagent), isopropanol (analytical reagent), and formic acid (analytical reagent) were purchased from Chengdu Kelong Chemical Reagent Factory (China); Deionized water was self-made; Sulfur (industrial grade) was from Yisheng New Material Co., Ltd. (China); Zinc oxide (industrial grade) was produced by

Dalian Zinc Oxide Co., Ltd. (China); stearic acid (SA) was purchased from Taike Browning Co., Ltd (China); antioxidant N-isopropyl-N'-phenyl-4-phenylenediamin (4010NA) was purchased from Sinopec Group Nanjing Chemical Industry Co., Ltd (China); vulcanization accelerator (CZ) was supplied by Kemai Chemical Co., Ltd. (China).

2.2. Preparation of TiO_2-CNTs nanoparticles

First, 109.2 mL deionized water and 10.8 mL isopropanol were mixed in a 250 mL flask. Then, CNTs were added into the mixed solution containing isopropanol. After being stirred for 2 h, the CNTs solution was obtained. Next, 13.6 mL titanium isopropanol was slowly added to the CNTs solution through the separating funnel, and the dripping time was about 30 min. Then, the hydrolysis reaction was maintained for 2 h at room temperature, accompanied by stirring. Afterwards, the product was washed with absolute ethanol and deionized water, and then the washed products were put into a vacuum oven and dried at 80 ℃ for 5 h. Finally, the TiO_2-CNTs nanoparticles were obtained.

2.3. Preparation of NR/TiO_2-CNTs nanocomposites

NR/TiO_2-CNTs composites were prepared by adding different contents of TiO_2-CNTs into NR latex, as shown in **Table 1**. Firstly, TiO_2-CNTs nanoparticles were added into a large beaker containing 200 ML deionized water. After stirring for 1 h and a following ultrasonic treatment for 2 h, the latex was slowly added into the beaker and stirred for 3 h. Here, the sonication power was 300W. Then, formic acid solution was slowly incorporated in the mixed solution until it was completely demulsified and settled. Then rubber composites were cut into small pieces and washed it with deionized water and ethanol until the formic acid was completely removed. Finally, these small pieces were put into a vacuum oven and dried at 80 ℃ for 12 h, and then NR/TiO_2-CNTs nanocomposites were obtained. Finally, different NR/TiO_2-CNTs nanocomposites were mechanically blended with vulcanizing agent, curing agent, and other additives by an open mixer. During mixing, the speed of mill was 60 rpm and

nip gap of the mill was 0.5 mm. After blending, these rubber composites were vulcanized by a flat curing machine (Qingdao Yadong Rubber Machinery Co. Ltd., China) at 150 ℃ and then continued pressing for 5 min at room temperature to hold their shape. Here, the curing time (10 min) was determined by t_{90}. In hydraulic heating press, the pressure was 15 MPa; the size of the mold was 100 mm × 100 mm × 2 mm. Finally, the vulcanized NR/TiO_2-CNTs plates was tailored by specific cutter according to the test standards. In addition, the 50 phr carbon black enhanced NR composites which are used for friction test were also prepared according to the same procedure as that mentioned above.

Table 1. The formulation of the composites.

Materials	**Additive contents (phr*)**				
NR	100	100	100	100	100
TiO_2-CNTs	1	2	3	5	7
Stearic acid	1	1	1	1	1
Zinc oxide	5	5	5	5	5
4010NA	2	2	2	2	2
CZ	1.5	1.5	1.5	1.5	1.5
Sulfur	2	2	2	2	2

*The number in the front of materials represent its content, and the unit is phr.

2.4. Measurements

Thermogravimetric analysis (TGA) was carried out on a thermal analyzer (NETZSCH, TG209, Germany) under the nitrogen/air atmosphere, and the heating rate was 10 ℃/min. Mechanical properties of NR and NR/TiO_2-CNTs composites were measured by a mechanical test machine (Instron 3366, USA) according to the standard GB/T 528-2009. Friction test was performed on a friction test machine (UMT-TriboLab, Bruke USA), and the applied rotating speed and pressure are 1800 rpm and 500 N during the friction time of 30 s, respectively. Rebound resilience property, hardness, and abrasion tests of NR and NR/TiO_2-CNTs composites were measured according to the standard GB/T 1681, GB/T

9867, and GB/T 531, respectively. Compression recovery ratios of NR and NR/TiO_2-CNTs composites were performed according to the GB/T 7759, and the compression set, compression time, and temperature are 25%, 24 h, and 100 ℃, respectively. Infrared thermal imager (FTLR T420) was used to track the temperature at the surface of samples. The surface morphology was examined by a scanning electron microscopy (SEM) (JEOL JSM 5900LV, Japan) and a Karl Zeiss LSM 800 Confocal Microscope (LSM800 Carl Zeiss Germany). In the SEM test, the used accelerating voltage is 10 kV. An X-ray energy dispersion spectrum (EDX) analyzer (Inca Penta-Fetx3 Oxford, USA) was used to measure the element contents of different samples. Transmission electron microscopy (TEM, model H-800, Hitachi, Japan) test of nanoparticles was completed at an accelerating voltage of 200 kV. FTIR spectra in the 4000-400 cm^{-1} was recorded by using a Nicolet 6700 spectrometer (Thermo Fisher Scientific, USA). X-ray diffraction (XRD) patterns were recorded by a DX-1000 X-ray diffractometer (PANalytical B.V., Holland) in the 2θ range of 5-80° by using Cu-Kα radiation (λ = 1.542 Å). A SPEX Raman apparatus (1403, USA) was used to record the laser Raman spectroscopy (LRS) in the scanning range of 500-2200 cm^{-1} using the excitation wavelength of 532 nm.

3. Results and discussion

3.1. Structural characterization of TiO_2-CNTs

SEM micrographs of CNTs, TiO_2, and TiO_2-CNTs are shown in **Figure 1**. The surface of CNTs is quite smooth. From **Figure 1b**, it can be found that there are many TiO_2 particles, and these particles agglomerate together. After hybridizing with CNTs by using TiO_2, many small TiO_2 particles adhere at the surface of CNTs, and some of them also aggregate at the outer wall. To clearly illustrate the microstructure, TEM test was used to further analyze CNTs and TiO_2-CNTs. **Figure 1d** shows that the surface of CNTs is very smooth, which is consistent with that shown in **Figure 1a**. For TiO_2-CNTs, the tubular structure can be clearly seen, for which inner tube is CNTs and outer particles are TiO_2.

According to SEM and TEM results, it is known that TiO_2 particles were formed at the surface of CNTs via a dehydration condensation process. In addition, EDX test was performed to illustrate the component of TiO_2-CNTs. According to **Figure 1f**, the TiO_2-CNTs are mainly consisted of C, O, and Ti elements, which further illustrates that the hybrid TiO_2-CNTs was formed.

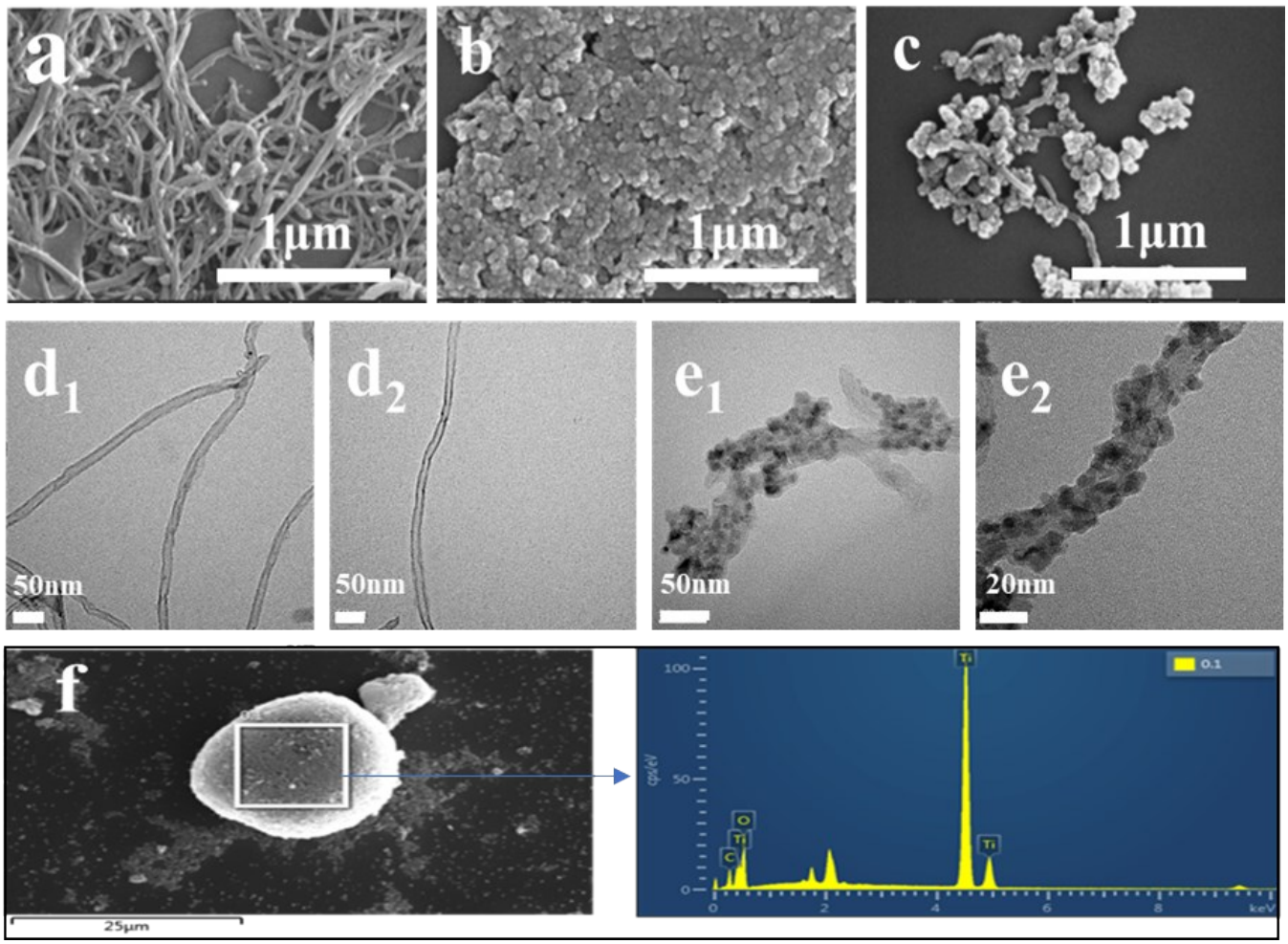

Figure 1. SEM micrographs of CNTs (a), TiO_2 (b), and TiO_2-CNTs (c); TEM micrographs of CNTs (d_1, d_2) and TiO_2-CNTs (e_1, e_2); EDX spectra of TiO_2-CNTs (f).

The prepared TiO_2-CNTs were further characterized by XRD. The result is shown in **Figure 2**. For CNTs, the diffraction peak at $2\theta = 26°$ is ascribed to the (002) reflection of CNTs. When CNTs are hybridized by TiO_2, several new peaks appear at $2\theta = 25.2°$, 37.8°, 48.1°, 53.9°, 55.1°, and 62.7° besides those ascribed to CNTs, corresponding to (101), (004), (200), (105), (211), and (204) crystal planes of anatase TiO_2 [17]. The XRD result indicates that the crystalline structures of both TiO_2 and CNTs were

not affected by the hybridizing reaction between them. In order to further illustrate the structure of TiO_2-CNTs, Raman test was performed for CNTs and TiO_2-CNTs. The results are shown in **Figure 3**. In Raman spectra, two absorption peaks located at about 1342 and 1576 cm^{-1} correspond to D and G bands of graphitized carbon [18]. The intensity ratio of D to G bands (I_D/I_G) can be used to characterize the change of defect degree of CNTs. The I_D/I_G for CNTs is 0.919, only slightly higher than 0.835 for TiO_2-CNTs, showing no significant change in the graphitization degree of CNTs. Clearly, the graphitization of CNTs was not remarkably affected by the hybridizing reaction with TiO_2.

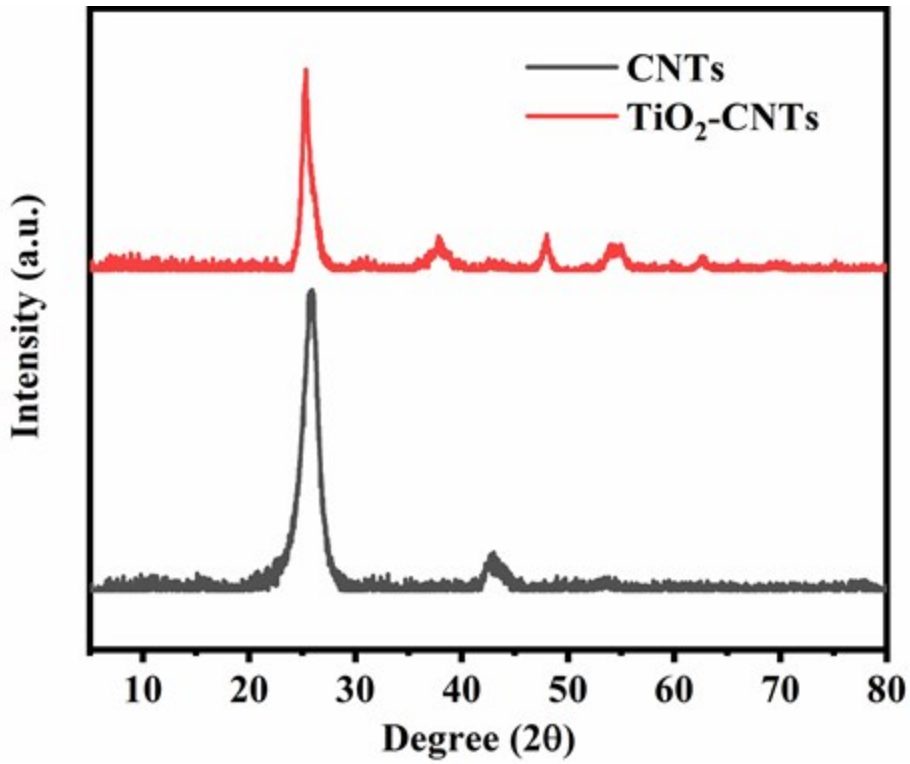

Figure 2. XRD patterns of CNTs and TiO_2-CNTs.

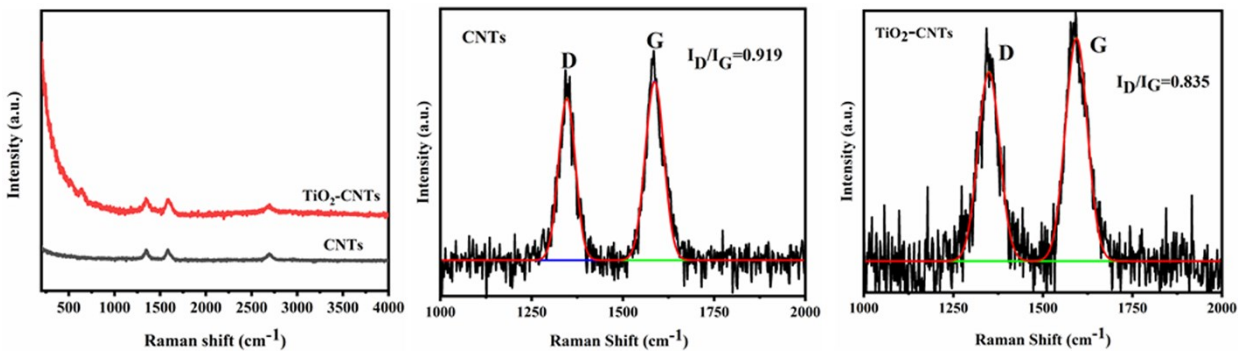

Figure 3. Raman spectra of CNTs and TiO_2-CNTs.

3.2. Thermal properties of CNTs and TiO_2-CNTs

TGA test was used to further characterize the thermal properties of TiO_2-CNTs. The result is shown in **Figure 4.** As a comparison, CNTs were also analyzed by TGA. Both TiO_2-CNTs and CNTs show only one decomposition stage from 40 to 700 ℃ under air atmosphere, and their initial decomposition temperatures have no apparent difference. For CNTs, the residue at 700 ℃ is significantly lower than that of TiO_2-CNTs, which should be due to the oxidation of CNTs. For TiO_2-CNTs, the initial decomposition temperature is close to that of CNTs. However, the residual mass of TiO_2-CNTs is significantly higher than that of CNTs, which is mainly due to the high residual mass of TiO_2 at high temperature [16]. Here, the mass percentage plot of CNT shows an upside trend after 650 ℃, which should be due to the unstable gas flow after 650 ℃. Obviously, the prepared TiO_2-CNTs possessed high thermal stability.

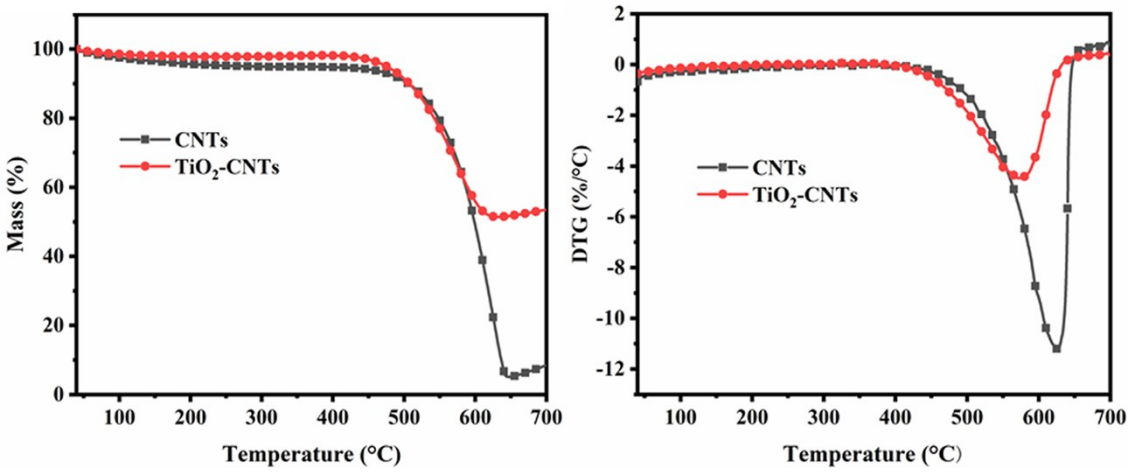

Figure 4. TG (a) and DTG (b) results of CNTs and TiO_2-CNTs.

3.3. Thermal properties of NR/TiO_2-CNTs composites

TGA results of different NR/TiO_2-CNTs composites are shown in **Figure 5** and **Table 2**. The $T_{5\%}$ and T_{max} are the decomposition temperature at 5 wt% mass loss and the decomposition temperature at the maximum mass loss rate, respectively. MLR_{max} is the maximum mass loss rate. In nitrogen atmosphere, the initial decomposition temperature of NR/1TiO_2-CNTs is 332.1 ℃, increased by 24 ℃

compared with that of NR. Clearly, a small amount of TiO_2-CNTs significantly improved the thermal stability of NR. The initial decomposition temperature of NR/TiO_2-CNTs gradually increases with raising the content of TiO_2-CNTs. However, the change of the temperature increment is quite low with increasing the TiO_2-CNTs content from 1 to 5 phr. According to previous studies [19-21], it can be concluded that the increase of initial decomposition temperature of NR after incorporation of the TiO_2-CNTs should mainly be attributed to the thermal conductivity and physical isolation of the TiO_2-CNTs. At 700 ℃, the residual mass of NR/TiO_2-CNTs containing 1-5 phr TiO_2-CNTs is higher than that of NR, which should be due to the higher residual mass of TiO_2-CNTs than that of NR. In addition, the decomposition rates of NR/TiO_2-CNTs composites at the maximum decomposing temperature have no apparent change compared with that of NR. In air atmosphere, both NR/TiO_2-CNTs composite and NR show two decomposition stages. For them, the additional decomposition at about 550 ℃ is ascribed to the change of hydrocarbons [7, 22, 23]. However, both NR/TiO_2-CNTs composites and NR have no an apparent difference in thermal stability in this case.

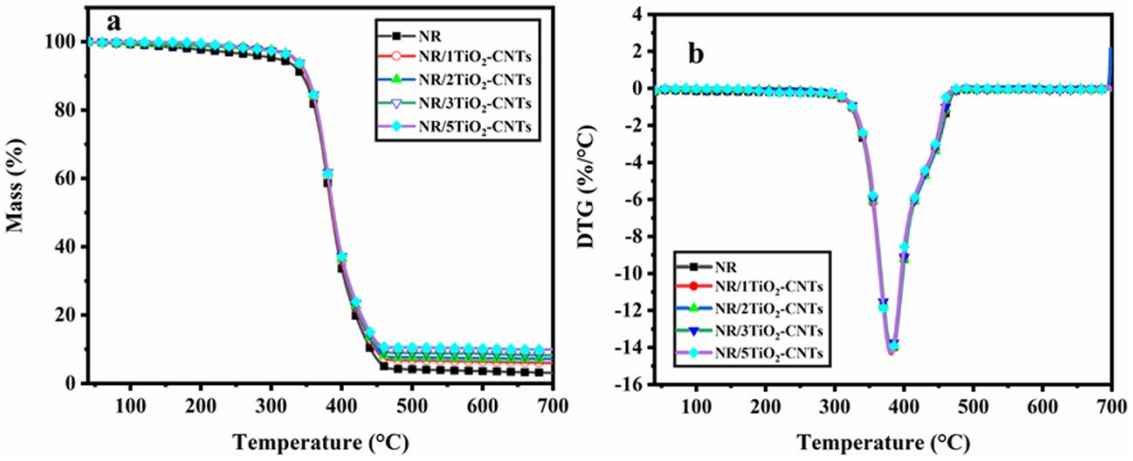

Figure 5. TG (a) and DTG (b) curves of NR/TiO_2-CNTs composites in N_2 atmosphere.

Table 2. Detailed TG data of NR/TiO_2-CNTs composites in N_2 atmosphere

Samples	$T_{5\%}$ (℃)	T_{max} (℃)	MLR_{max} (%/℃)	Residue (%)
NR	308.8	381.4	14.3	3.2
NR/1TiO_2-CNTs	332.1	381.1	14.3	6.0

NR/2TiO_2-CNTs	334.4	381.6	14.2	7.2
NR/3TiO_2-CNTs	334.3	381.5	14.0	8.3
NR/5TiO_2-CNTs	333.7	381.1	14.3	10.0

3.4. Mechanical properties of NR/TiO_2-CNTs composites

The elastic modulus at break, tensile strength, and elongation at break for NR and NR/TiO_2-CNTs composites are shown in **Figure 6.** Basically, these properties for all NR/TiO_2-CNTs composites containing 1, 2, 3, and 5 phr TiO_2-CNTs are superior to those of NR composites, and all of them firstly increase to a maximum value and then decrease, showing a similar change trend with raising the content of TiO_2-CNTs. For NR composite, the elastic modulus, tensile strength, and elongation at break are 2.9 MPa, 19.2 MPa, and 1395.1%, respectively. When the TiO_2-CNTs is 3 phr, all of them for NR/3TiO_2-CNTs respectively reach 4.1 MPa, 32.0 MPa, and 1604.1%, correspondingly increased by 41.4%, 66.7%, and 15.0%. In this case, the tensile strength of NR/3TiO_2-CNTs almost reaches the maximum value, which is equivalent to the strength of 50 phr carbon black filled NR composite (about 32.0 MPa in our experiment). The elongation at break for NR/1TiO_2-CNTs and elastic modulus for NR/5TiO_2-CNTs are slightly higher than the corresponding values of other NR/TiO_2-CNTs composites in the TiO_2-CNTs range from 0 to 9 phr, respectively. Clearly, the TiO_2-CNTs is an ideal reinforcing agent for NR, and a small amount of TiO_2-CNTs may significantly enhance the mechanical properties of NR.

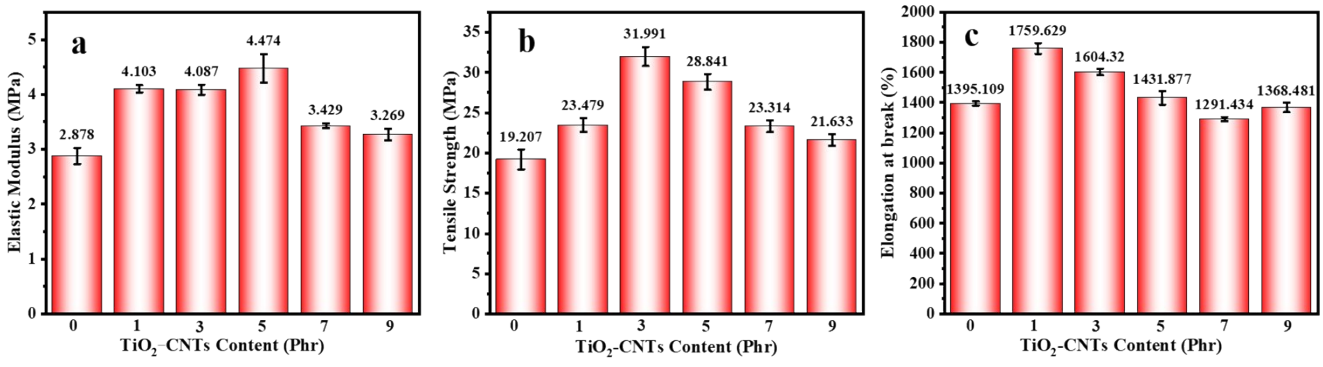

Figure 6. Mechanical properties of NR and NR/TiO_2-CNTs composites: elastic modulus (a), tensile

strength (b), and elongation at break (c).

3.5. Rebound resilience, abrasion, compression properties, and hardness

Table 3 shows that the hardness and rebound resilience of NR increase slightly after incorporation of the TiO_2-CNTs. When the content of TiO_2-CNTs is 5 phr, the hardness and rebound resilience of NR/5TiO_2-CNTs raise to 40.6 HA and 71.5%, respectively. For compression recovery ratio, there is no apparent change with increasing the TiO_2-CNTs from 1 to 5 phr compared with that of NR. As for abrasion property, it can be found that the abrasion indexes of NR composites show slight fluctuation in comparison with that of NR when there are only 1 and 2 phr TiO_2-CNTs. With increasing the TiO_2-CNTs to 3 and 5 phr, the abrasion indexes of NR/3TiO_2-CNTs reach 143.1 and 158.6%, respectively. Clearly, TiO_2-CNTs has different influences on the rebound resilience, abrasion, compression properties, and hardness of NR.

Table 3. The hardness, rebound resilience, abrasion, and compression properties of the composites

Samples	NR	NR/1TiO_2-CNTs	NR/2TiO_2-CNTs	NR/3TiO_2-CNTs	NR/5TiO_2-CNTs
Abrasion index (%)	132.5±31.1	129.6±10.2	125.5±2.8	143.1±15.7	158.6±31.6
rebound resilience (%)	62.3±0.9	65.9±0.5	66.9±0.2	71.2±1.2	71.5±0.5
Compression recovery ratio (%)	59.9±4.2	56.1±0.8	63.1±2.9	60.3±3.7	59.3±1.6
Hardness (HA)	36.6±1.2	39.2±0.8	40.2±2.1	40.9±2.3	40.6±1.5

3.6. The vulcanization properties of NR/TiO_2-CNTs composites

The vulcanization properties of different NR/TiO_2-CNTs composites are shown in the **Figure 7**. Compared to NR composite, the addition of TiO_2-CNTs makes the torque of composite increase to some

extent, suggesting that TiO_2-CNTs efficiently increased the crosslink density of composites. Here, the increased crosslink density is mainly ascribed to the physical crosslinking caused by nanoparticles. When the addition amount of TiO_2-CNTs is 3 or 5 phr, the torque of composite decreases slightly, which should be attributed to the aggregation of TiO_2-CNTs in the matrix.

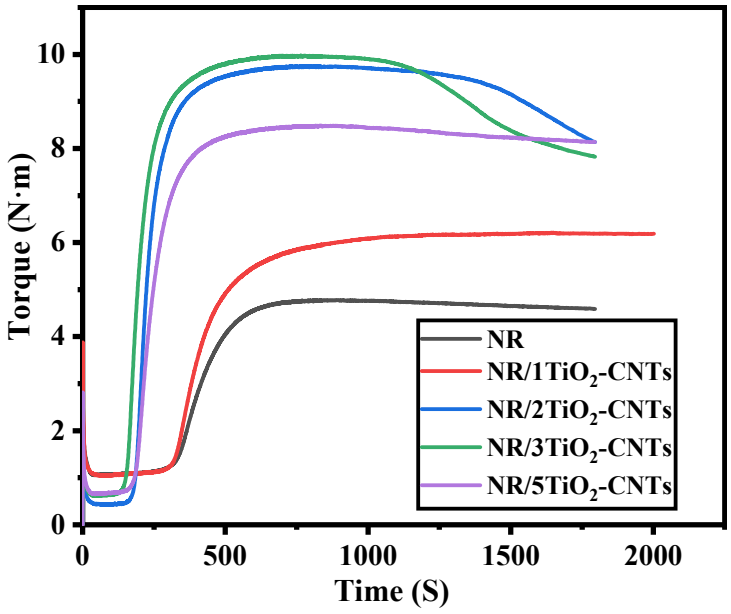

Figure 7. Vulcanization properties of different NR/TiO_2-CNTs composites.

3.7. High-temperature stability of NR/TiO_2-CNTs composites under extreme friction condition

The temperature change at the friction surface of NR/TiO_2-CNTs composites was observed by Infrared thermal imager. **Figure 8** shows the highest temperature of the friction surface of NR/TiO_2-CNTs composites in 30 s during the friction test. Here, it should be noted that the friction test was performed in the presence of 50 phr carbon black in NR composite. The maximum temperatures at the friction surfaces of NR and NR/1TiO_2-CNTs are 246 ℃, but the maximum temperatures at the friction surfaces of NR/3TiO_2-CNTs and NR/5TiO_2-CNTs decrease compared with that of NR, which are 217 ℃ and 210 ℃, respectively, correspondingly decreased by 29 and 36 ℃ compared with that at the surface of NR. However, there is no apparent change in the friction time to reach the maximum temperature at the friction surface between NR and NR/TiO_2-CNTs composites. The above experimental results showed that a small amount of TiO_2-CNTs reduced the temperature peak at the

friction surface of NR, which remarkably enhanced the stability of the tread of aircraft tires when experiencing the extreme friction condition. Here, the low heat signature was detected on the surface of NR/TiO_2-CNTs composites, which should mainly be due to the reduction of surface friction or the higher thermal conductivity. Of course, thermal stability of NR/TiO_2-CNTs composites also play a role in decreasing the surface temperature.

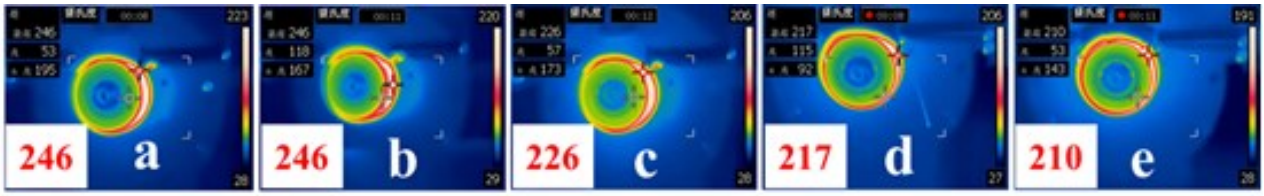

Figure 8. The maximum temperatures at the surfaces of NR (a), NR/1TiO_2-CNTs (b), NR/2TiO_2-CNTs (c), NR/3TiO_2-CNTs (d) and NR/5TiO_2-CNTs (e) during the friction test.

3.8. Mechanisms for mechanical enhancement and the improved high-temperature stability

First, the brittle-fractured surfaces of NR and NR/TiO_2-CNTs composites were investigated by SEM, and the result is shown in **Figure 9**. When the amount of TiO_2-CNTs is 3 phr, the bulge of a single nanotube can be seen locally, which should be caused by the insertion of nanotubes. At 3 phr TiO_2-CNTs in NR, the micro aggregation of nanotubes appears. In order to more directly observe the dispersion of TiO_2-CNTs in NR substrate, TEM test was performed for NR and NR/TiO_2-CNTs composites. For NR, there are some black particles (marked by red ellipse), which should be from insoluble sulfur that is dispersed in NR substrate. For the composites filled with different amounts of TiO_2-CNTs, nanotubes (marked by blue ellipse) can be clearly seen in NR matrix. When the loading amount of TiO_2-CNTs is 1 phr, the nanotubes do not agglomerate obviously, and the dispersion of TiO_2-CNTs is very uniform. With increasing the TiO_2-CNTs to 3 phr, slight agglomeration for nanotubes appears. When the content of TiO_2-CNTs reaches 5 phr, some big aggregates exist in NR. These results indicate that it is very easy to agglomerate for TiO_2-CNTs in NR matrix when the amount of TiO_2-

CNTs is higher than 3 phr, which should be an important reason to affect the mechanical properties.

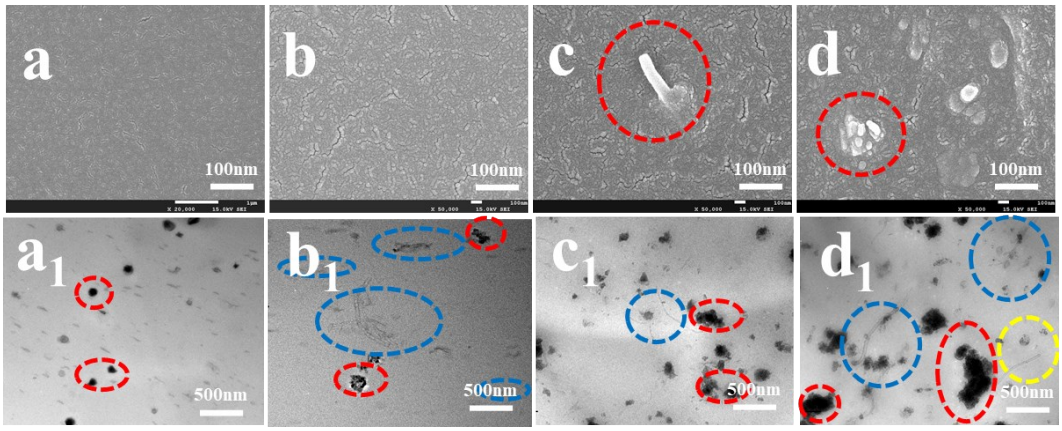

Figure 9. SEM and TEM micrographs of NR and NR/TiO_2-CNTs composites: NR (a, a_1), NR/1TiO_2-CNTs (b, b_1), NR/3TiO_2-CNTs (c, c_1), NR/5TiO_2-CNTs (d, d_1).

Figure 10 shows SEM micrographs at the friction surfaces of NR and NR/TiO_2-CNTs composites after the friction test. The result shows that there are obvious cavities at the friction surface of NR, and there are some debris at the edge of the cavities. For NR/1TiO_2-CNTs and NR/2TiO_2-CNTs composites, there are also some cavities and debris at the friction surfaces. However, no cavity or debris can be observed at the friction surface for NR/3TiO_2-CNTs, the friction surface is continuous and dense, showing a toughness characteristic. At 5 phr TiO_2-CNTs, there are a small amount of cracks at the surface of NR/5TiO_2-CNTs composite. Moreover, some aggregates also exist at the surface, which should be related to the aggregation of TiO_2-CNTs, which is consistent with the SEM result shown in **Figure 9**. Analysis for the morphology of the friction surface demonstrated that the introduction of TiO_2-CNTs affected the friction behavior of NR and reduced the damage of friction to the surface of NR, which should be an important reason for the improved stability of NR/TiO_2-CNTs composites containing a small amount of TiO_2-CNTs.

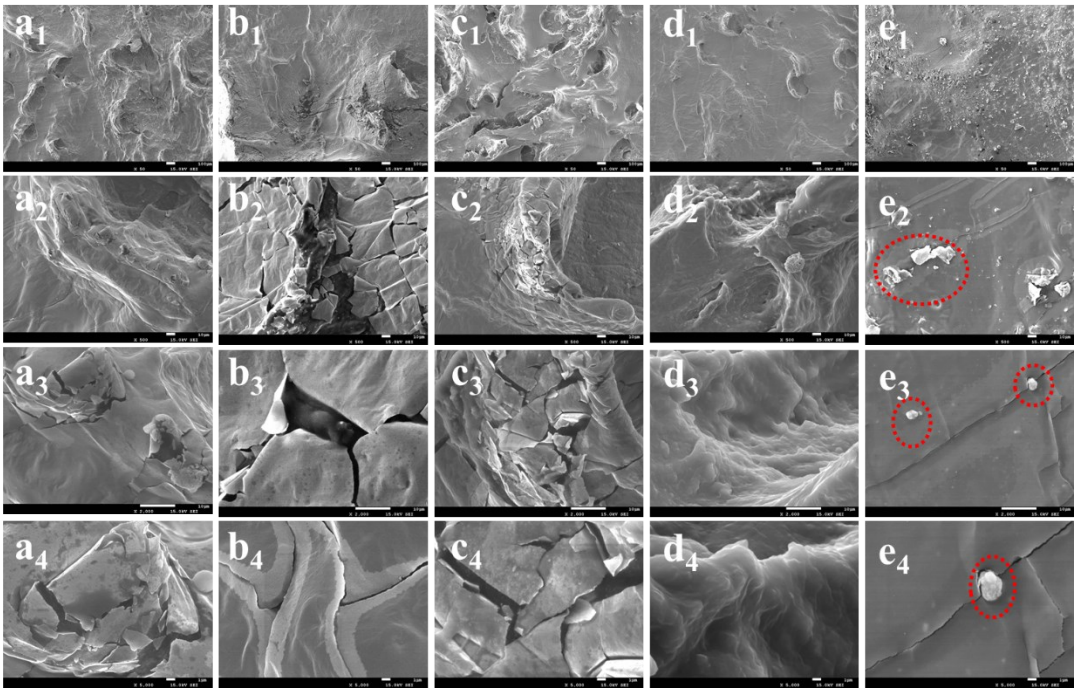

Figure 10. SEM micrographs at the friction surfaces of NR (a_1, a_2, a_3, a_4), NR/1TiO_2-CNTs (b_1, b_2, b_3, b_4) , NR/2TiO_2-CNTs (c_1, c_2, c_3, c_4) , NR/3TiO_2-CNTs (d_1, d_2, d_3, d_4), and NR/5TiO_2-CNTs (e_1, e_2, e_3, e_4).

Confocal microscope was also used to analyze the friction surface of different rubber composites, and the morphologies and roughness data of different friction surfaces are respectively shown in **Figure 11** and **Table 4**. The result shows that the roughness of friction surface decreases with the increase of TiO_2-CNTs. When the contents of TiO_2-CNTs are 3 and 5 phr, the roughness data at the corresponding friction surfaces are reduced to 8.2 and 3.8 μm, much lower than that of NR, which must be an important reason for the obvious decrease in the maximum temperature at the friction surfaces of NR/3TiO_2-CNTs and NR/5TiO_2-CNTs.

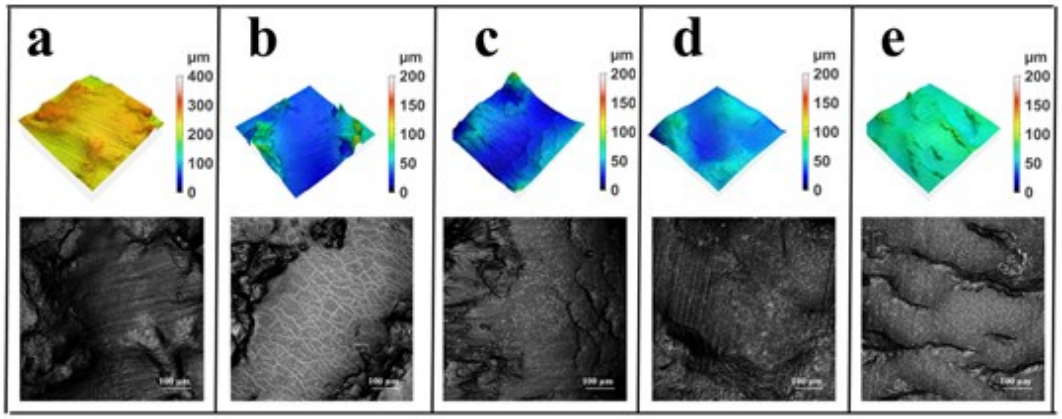

Figure 11. Confocal microscope pictures of the friction surfaces of NR (a), NR/1TiO_2-CNTs (b), NR/2TiO_2-CNTs (c), NR/3TiO_2-CNTs (d), and NR/5TiO_2-CNTs (e).

Table 4. Roughness data at the friction surfaces of NR/TiO_2-CNTs composites after the friction test

Samples	NR	NR/1TiO_2-CNTs	NR/2TiO_2-CNTs	NR/3TiO_2-CNTs	NR/5TiO_2-CNTs
Sa* (μm)	13.3	11.6	10.6	8.2	3.8

* Sa is the index to evaluate roughness.

Figure 12 shows EDS result at the friction surfaces of NR and NR/TiO_2-CNTs composites after the friction test. When the TiO_2-CNTs are incorporated into NR, the relative contents of C, O, and S elements at the friction surface change significantly. The relative content of S element at the friction surface of NR/1TiO_2-CNTs, NR/2TiO_2-CNTs, or NR/3TiO_2-CNTs decreases compared with that of NR, and the relative content of O element also decreases, while the relative content of C increases in this case. It is worth noting that the relative content of O element at the friction surface of NR/5TiO_2-CNTs is relatively high, which should be caused by the presence of more TiO_2-CNTs at the surface, as illustrated in SEM results shown in **Figure 9** and **10**. On the basis of less O element and more C element at the friction surfaces of NR/1TiO_2-CNTs, NR/2TiO_2-CNTs, and NR/3TiO_2-CNTs composites, it can be concluded that the damage of friction to crosslinking network of NR was reduced when a small

amount of TiO_2-CNTs was incorporated into NR, further illustrating that a small amount of TiO_2-CNTs promoted the stability of NR under the intensive friction condition.

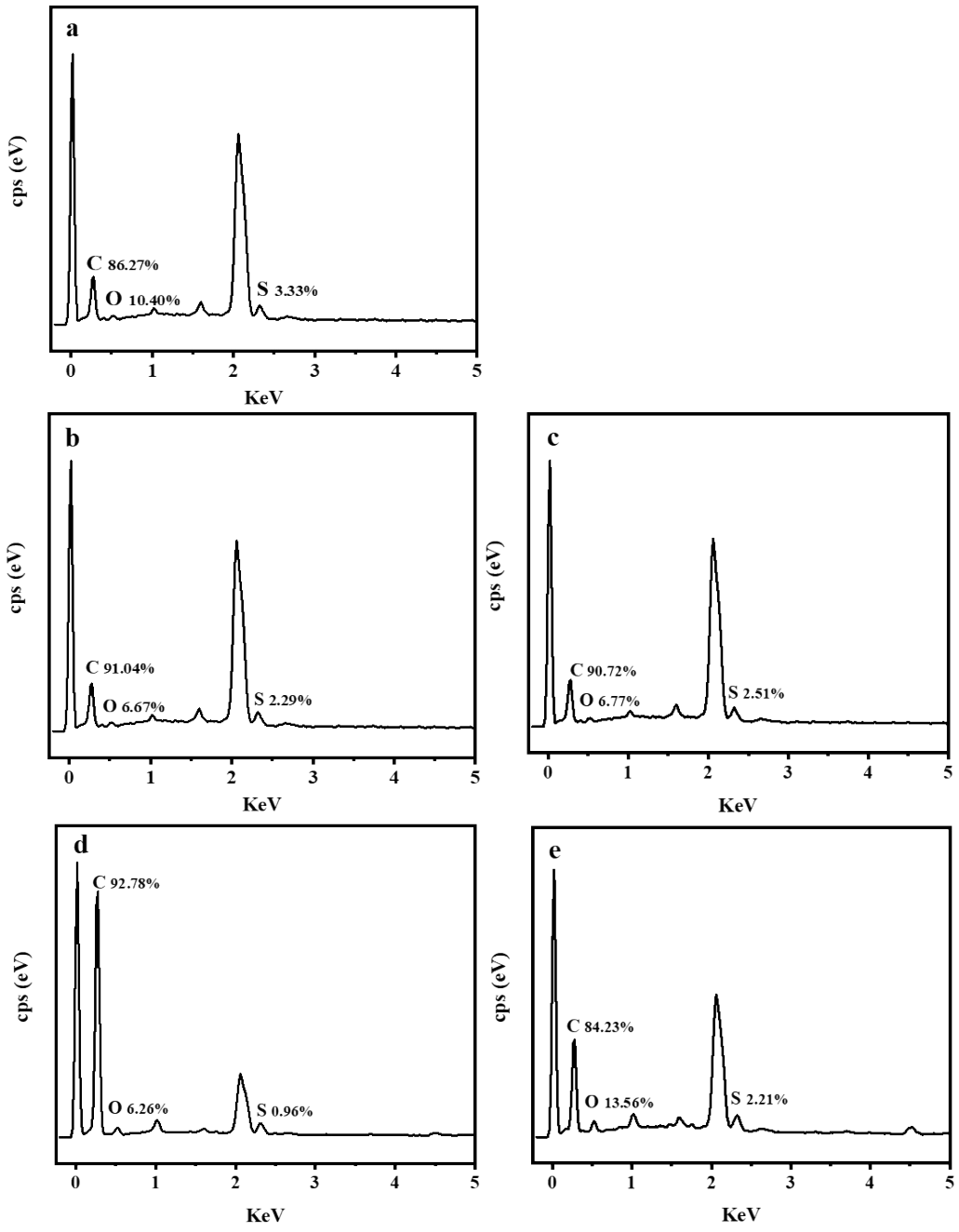

Figure 12. EDS result at the friction surfaces of NR(a), NR/1TiO_2-CNTs (b), NR/2TiO_2-CNTs (c), NR/3TiO_2-CNTs (d), and NR/5TiO_2-CNTs (e).

In order to further study the high-temperature stability of NR/TiO_2-CNTs composites, LRS test was used to study the difference in graphitization degree at the friction surface for NR and NR/TiO_2-CNTs composites. The result is shown in **Figure 13**. For NR, the I_D/I_G value of the material at the

friction surface is 5.85. After incorporation of 1 phr TiO_2-CNTs, the I_D/I_G value decreases slightly. With the increase of TiO_2-CNTs, the I_D/I_G value at the surface of NR/TiO_2-CNTs composites decreases gradually, and it greatly reduces to 3.85 when TiO_2-CNTs is 5 phr, which is significantly lower than that of NR, indicating that the TiO_2-CNTs promoted the graphitization degree at the friction surface of NR during the friction test. The graphitization degree at the friction surface can protect the internal substrate more effectively and prevent the erosion of heat and oxygen. Consequently, a small amount of TiO_2-CNTs made a positive contribution to the high-temperature stability of NR/TiO_2-CNTs composites via promoting the graphitization degree at the friction surface of NR.

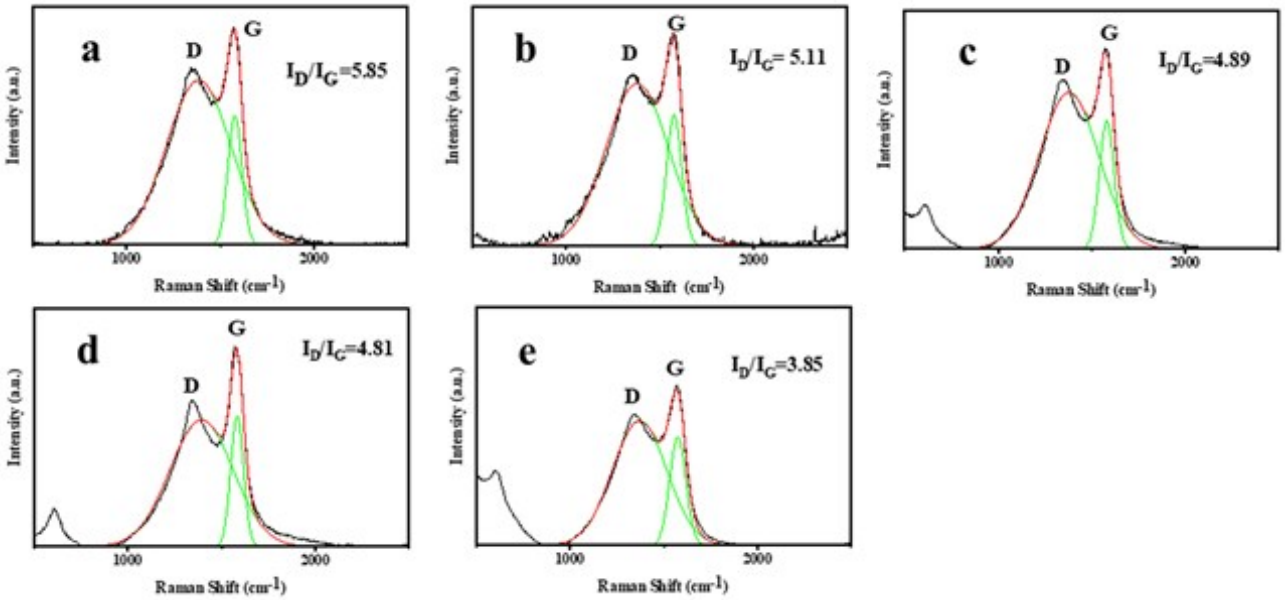

Figure 13. Raman spectra of the friction surfaces of NR (a), NR/1TiO_2-CNTs (b), NR/2TiO_2-CNTs (c), NR/3TiO_2-CNTs (d), and NR/5TiO_2-CNTs (e).

4. Conclusions

TiO_2-CNTs hybrid was prepared by the sol-gel method the in current work. Different measurements demonstrated that TiO_2-CNTs have the tubular structure, for which inner tube is CNT and outer particles are TiO_2. When the TiO_2-CNTs were used to fabricate NR/TiO_2-CNTs composites, it was found that only 3.0 wt% of TiO_2-CNTs endowed NR with significantly improved tensile strength

and elastic modulus, which are 32.0 MPa and 4.1 MPa, respectively, correspondingly increased by 66.7% and 41.4% compared with that of NR. More importantly, the stability of NR under extreme friction condition was greatly improved. The maximum temperatures at the friction surfaces of NR/3TiO_2-CNTs and NR/5TiO_2-CNTs were greatly reduced by 29 and 36 ℃ compared with that for NR. The mechanisms for the mechanical enhancement of NR and the improved stability of NR/TiO_2-CNTs composites under extreme friction condition were deeply discussed. All these experimental results demonstrated that the hybridization of both TiO_2 and CNTs may efficiently simultaneously achieve mechanical enhancement of natural rubber and its stability under extreme friction condition, and the TiO_2-CNTs have a potential value in the tread material of aircraft tires.

Acknowledgements

This work was supported by the National Natural Science Foundation of China (No. 51790504, 51673132, 51827803, and 51991351)

References

[1] M.J. Matheson, T.P. Wampler, W.J. Simonsick, The effect of carbon-black filling on the pyrolysis behavior of natural and synthetic rubbers, Journal of Analytical and Applied Pyrolysis 29(2) (1994) 129-136.

[2] S. Straus, S.L. Madorsky, Thermal degradation of unvulcanized and vulcanized rubber in a vacuum, Industrial and Engineering Chemistry 48(7) (1956) 1212-1219.

[3] D.D. Jiang, G.F. Levchik, S.V. Levchik, C. Dick, J.J. Liggat, C.E. Snape, C.A. Wilkie, Thermal degradation of cross-linked polyisoprene and polychloroprene, Polymer Degradation and Stability 68(1) (2000) 75-82.

[4] J.W. Hao, C.A. Wilkie, J.Q. Wang, An XPS investigation of thermal degradation and charring of cross-linked polyisoprene and polychloroprene, Polymer Degradation and Stability 71(2) (2001) 305-

315.

[5] D.W. Brazier, G.H. Nickel, Thermoanalytical methods in vulcanizate analysis .1. differential scanning calorimetry and heat of sulfur vulcanization, Rubber Age 106(9) (1974) 52-53.

[6] J. Xigao, L. Huiming, Determination of the cross-link density of vulcanized polyisoprene by pyrolysis-gas chromatography-mass spectrometry, Journal of Analytical and Applied Pyrolysis 3(1) (1981) 49-57.

[7] F.Z. Chen, J.L. Qian, Studies on the thermal degradation of cis-1,4-polyisoprene, Fuel 81(16) (2002) 2071-2077.

[8] R.S.L. Sally A.Groves, MarianneBlazsó,TamásSzékely, Natural rubber pyrolysis: Study of temperature-and thickness-dependence indicates dimer formation mechanism, Journal of Analytical and Applied Pyrolysis 19 (1991) 301-309.

[9] H. Pakdel, D.M. Pantea, C. Roy, Production of dl-limonene by vacuum pyrolysis of used tires, Journal of Analytical and Applied Pyrolysis 57(1) (2001) 91-107.

[10] J.C.W.ChienJ.K.Y.Kiang, Polymer reactions—X thermal pyrolysis of poly(isoprene), European Polymer Journal 15(11) (1979) 1059-1065.

[11] S. Khanlari, M. Kokabi, Thermal Stability, Aging Properties, and Flame Resistance of NR-Based Nanocomposite, Journal of Applied Polymer Science 119(2) (2011) 855-862.

[12] G. Sui, W. Zhong, X.P. Yang, Y. Yu, S. Zhao, Preparation and properties of natural rubber composites reinforced with pretreated carbon nanotubes, Polymers for Advanced Technologies 19(11) (2008) 1543-1549.

[13] M.A. Lopezmanchado, J. Biagiotti, L. Valentini, J.M. Kenny, Dynamic mechanical and Raman spectroscopy studies on interaction between single-walled carbon nanotubes and natural rubber, Journal of Applied Polymer Science 92(5) (2004) 3394-3400.

[14] N. Hayeemasae, H. Ismail, S. Matchawet, A. Masa, Kinetic of thermal degradation and thermal stability of natural rubber filled with titanium dioxide nanoparticles, Polymer Composites 40(8) (2019) 3149-3155.

[15] J. Gong, R. Niu, N. Tian, X.C. Chen, X. Wen, J. Liu, Z.Y. Sun, E. Mijowska, T. Tang, Combination of fumed silica with carbon black for simultaneously improving the thermal stability, flame retardancy and mechanical properties of polyethylene, Polymer 55(13) (2014) 2998-3007.

[16] L. Bai, X. Wang, J. Tan, H. Li, J. Zheng, Study of distinctions in the synergistic effects between carbon nanotubes and different metal oxide nanoparticles on enhancing thermal oxidative stability of silicone rubber, Journal of Materials Science 51(15) (2016) 7130-7144.

[17] B. Gao, G.Z. Chen, G.L. Puma, Carbon nanotubes/titanium dioxide ($CNTs/TiO_2$) nanocomposites prepared by conventional and novel surfactant wrapping sol-gel methods exhibiting enhanced photocatalytic activity, Applied Catalysis B-Environmental 89(3-4) (2009) 503-509.

[18] N. Lachman, X. Sui, T. Bendikov, H. Cohen, H.D. Wagner, Electronic and mechanical degradation of oxidized CNTs, Carbon 50(5) (2012) 1734-1739.

[19] Y. Wang, X. Qiu, J. Zheng, Study the mechanism that carbon nanotubes improve thermal stability of polymer composites: An ingenious design idea with coating silica on CNTs and valuable in engineering applications, Composites Science and Technology 167 (2018) 529-538.

[20] M. Koc, Y. Aueulan, T. Altan, On the characteristics of tubular materials for hydroforming—experimentation and analysis, International Journal of Machine Tools & Manufacture 41(5) (2001) 761-772.

[21] T. Zribi, A. Khalfallah, H. Belhadjsalah, Experimental characterization and inverse constitutive parameters identification of tubular materials for tube hydroforming process, Materials & Design 49 (2013) 866-877.

[22] T. Midgley, A.L. Henne, Natural and synthetic rubber I Products of the destructive distillation of natural rubber, Journal of the American Chemical Society 51(1-4) (1929) 1215-1226.

[23] F. Cataldo, Thermal depolymerization and pyrolysis of cis-1,4-polyisoprene: preparation of liquid polyisoprene and terpene resin, Journal of Analytical and Applied Pyrolysis 44(2) (1998) 121-130.